

## Refractive or diffractive interpretation of heavy-ion elastic scattering

G. Madurga, A. Jadraque, and M. Lozano

Facultad de Física, Universidad de Sevilla, Sevilla 4, Spain

(Received 1 December 1980)

A characteristic pattern frequently observed in the angular distribution of heavy-ion elastic scattering at moderate energies above the Coulomb barrier has been attributed either to a Fresnel diffraction or to a rainbow effect. We propose a comparison between the strong absorption radius  $R_{sa}$  and the rainbow radius  $R_r$  at different energies, which may have some relevance on deciding whether the absorptive or the refractive interpretation is to be preferred. Despite the difficulties in the exact determination of these two distances, an analytical expression for their energy dependence is found empirically by analyzing data of fifteen pairs of heavy ions. According to this criterion the center-of-mass energy, above which refraction prevails over absorption, is proportional to  $Z_1 Z_2$ .

[NUCLEAR SCATTERING Optical and diffraction models, rainbow refraction of heavy ions.]

### I. INTRODUCTION

In today's language one could say that the first scattering experiments with nuclei, as interpreted by Rutherford, showed that the nucleus-nucleus potential is a Coulomb potential,<sup>1</sup>  $Z_1 Z_2 e^2 / r$ , at distances  $r > 10^{-12}$  cm, or equivalently that  $\sigma / \sigma_R = 1$ , with  $\sigma_R \propto [\sin(\theta/2)]^{-4}$ , for trajectories which imply internuclei distances of closest approach greater than the above mentioned limit. The energy and angle which mark the frontier of validity to the equivalence  $\sigma / \sigma_R = 1$  thus offered the first crude measurement of the nuclear size. The deflection function  $\theta(l)$ , for a charged particle with sufficient energy, scattered in the electrostatic field of an extended (not point) charge, has a maximum (or a minimum, for opposite charges)  $\theta_r^{(c)}$ , which implies a singularity in the classical cross section, or oscillations, an enhancement, and a sharp drop in the corresponding quantal cross section. This is called the *Coulomb rainbow*.

In addition to the electrostatic long-range repulsion the nucleus-nucleus interaction has a very strong attraction at distances of a few fm, and this can force the deflection function to go through a minimum<sup>2</sup>  $\theta_r^{(n)}$ , at smaller values of the orbital momentum. The corresponding cross section effect is called the *nuclear rainbow*.

For small projectiles ( $Z \leq 2$ ) the Coulomb potential is weak and the nuclear rainbow dominates,  $|\theta_r^{(n)}| > \theta_r^{(c)}$ , while the contrary is true for heavy ions. Goldberg<sup>3</sup> has stressed the need for experimental data up to angles beyond those corresponding to the nuclear rainbow if one has to determine unambiguously the optical potential for describing the alpha-nucleus elastic scattering. With Li, and possibly with Be also, a weak nuclear rainbow

can still be observed, but not with heavier projectiles. Indeed the strong absorption, typical of heavy ion collisions, enters into play rather sharply at a critical distance greater than the distance of closest approach corresponding to the nuclear rainbow trajectory, and the latter is prevented from contributing to the elastic scattering. Absorption is described in an optical model by means of an imaginary potential.

In the opinion of some authors<sup>3,4</sup> the Coulomb rainbow does seem to play a role in the elastic scattering of heavy ions at least at certain energies. Classically this is a refraction effect produced by the real part of the optical potential. In a quantal description, because of the blurring of the trajectory and interference effects, the rainbow angular distribution of  $\sigma / \sigma_R$  shows a series of oscillations with increasing amplitude followed by a quasiexponential fall into the classically forbidden (or shadow) region. A similar picture can be obtained, on the other hand, by the absorption sharp boundary with the contribution of the "diverging lens" effect produced by the strong Coulomb field, and this is called Fresnel diffraction. Frahn<sup>5</sup> and Fuller<sup>6</sup> hold that the analysis of the phase of the scattering amplitude rules out the rainbow interpretation. More recently, however, Satchler<sup>7</sup> considers that the question is not yet completely resolved whether such a pattern is due to the refractive effects of the real nuclear potential (i.e., whether it should be called rainbow scattering) or whether it is diffractive (i.e., whether it should be called Fresnel scattering) due to the sudden onset of strong absorption at the nuclear surface.

In this work we do not intend to solve the problem but only offer a comparison between an ab-

sorption distance and a rainbow distance which may have some bearing on it: One would think that whichever distance is greater will tend to make the corresponding effect prevail. Nevertheless, the definition of both distances, especially the rainbow one, are somehow tied to the classical concept of trajectory and the interplay between refractive and interference effects in both interpretations is too apparent for the argument to be conclusive.

The ambiguity in the definitions of these distances is described in Sec. II. A regular energy dependence of such distances is suggested in Sec. III. The criterion of Sec. II is applied to fifteen pairs of heavy ions in Sec. IV. Finally, a simple  $Z_1 Z_2$  dependence is found in Sec. V for the crossing energy above which refraction would dominate; some concluding remarks are summarized in Sec. VI. Energies are given in MeV and distances in fm throughout this work.

## II. STRONG ABSORPTION DISTANCE AND RAINBOW DISTANCE

There are in the literature many, not altogether equivalent, definitions designed to describe the internuclei distance at which the probability of a non-purely-elastic event becomes important.<sup>8</sup> Perhaps the most popular, and the one we use in this paper, is the strong absorption radius defined as the distance of closest approach of the Rutherford trajectory with 50% absorption. This definition mixes quantum and classical concepts: The scattering matrix  $S_l$  is computed for integer values of  $l$  by solving the Schrödinger equation with a complex potential; then a value  $l_{sa}$  is interpolated for which the partial wave (if it existed for noninteger  $l$ ) would have transmission coefficient  $T_{l_{sa}} = 1 - |S_{l_{sa}}|^2 = \frac{1}{2}$ ; and a classical trajectory is chosen with angular momentum  $l_{sa} + \frac{1}{2}$ , semiclassically corresponding<sup>9</sup> to the quantum orbital momentum  $l_{sa}$ . Then our strong absorption radius is

$$R_{sa} = \frac{\eta}{k} \left\{ 1 + \left[ 1 + \frac{(l_{sa} + \frac{1}{2})^2}{\eta^2} \right]^{1/2} \right\}, \quad (1)$$

with  $k = (2mE/\hbar)^{1/2}$  and  $\eta = Z_1 Z_2 e^2 / \hbar v$ .

Equation (1) neglects the effect of the nuclear potential on the trajectory. The nuclear potential is very weak for  $r > R_{sa}$  and usually causes no sensible change in this trajectory. In very few cases the exact (not Rutherford) trajectory corresponding to  $l_{sa} + \frac{1}{2}$  jumps inside the pocket, formed by the effective (real + centrifugal) potential, and reaches a distance of closet approach much shorter than (1). Such classical trajectory would be absorbed by the imaginary potential and

give no contribution to elastic scattering. It is reasonable therefore to use Eq. (1) rather than a more exact one which would be either equivalent or, when not, meaningless to our problem.

The strong absorption radius just defined depends on the real and imaginary parts of the optical potential fitted to the experimental data for a given pair of nuclei at a given energy. It is a well known feature of heavy ion elastic scattering that there is a large amount of ambiguity in the determination of the optical potential by the experimental data.<sup>8,10</sup> This ambiguity, at least with the sets of experimental data available today, implies fluctuations of say  $\pm 0.1$  fm in the values of  $R_{sa}$  obtained with potentials that fit the data with a  $\chi^2$  differing less than 1% from the best fit.<sup>8</sup> With less stringent fits the oscillations of  $R_{sa}$  are much larger.

The value of  $R_{sa}$  is known to decrease slowly with increasing energy for a given pair.<sup>11</sup> In particular for  $^{16}\text{O} + ^{208}\text{Pb}$  the value of  $R_{sa}$  at 192 MeV is 0.32 fm shorter than at 129.5 MeV, and this energy dependence is the same within  $\pm 0.02$  for other alternative definitions of a strong absorption radius considered in Ref. 8. We note that this change (0.32) is comparable with, and the fluctuation (0.02) substantially smaller than, the degree of indetermination one obtains when deriving  $R_{sa}$  from a particular fit to a given set of data. In this particular case we have determined  $R_{sa}$  as the central value among those corresponding to a large sample of good fits. But this procedure is not practical for a general study of the energy dependence of  $R_{sa}$  because of the amount of computing time required and because in many cases we do not have the numerical experimental data and must rely on the optical model fits published by other authors.

Consequently the comparison of the  $R_{sa}$  value at two different energies may not be meaningful if the two fits have been done with a different criterion: one with a shallow and the other with a deep potential; or one fits the depth with a given radius, while the other varies the radius with a fixed depth, etc.

As a measure of the distance at which rainbow refraction takes place we define a (Coulomb) rainbow distance as the distance of closest approach of the Rutherford trajectory corresponding to the rainbow angular momentum

$$R_r = \frac{\eta}{k} \left\{ 1 + \left[ 1 + \frac{(l_r + \frac{1}{2})^2}{\eta^2} \right]^{1/2} \right\}, \quad (2)$$

where  $l_r$  makes maximum the deflection function. Except for the semiclassical substitution  $l_r \rightarrow l_r + \frac{1}{2}$ , this definition is classical, and  $R_r$  depends only on the real part of the optical potential. The real

nuclear potential determines the rainbow orbital momentum  $l_r$ , but its effect in the trajectory is neglected in Eq. (2) for the same reasons we explained in the  $R_{sa}$  case.

The ambiguity of the optical potential implies a certain degree of indefiniteness in  $R_r$ , as in  $R_{sa}$ . Hence the general trend of a large amount of data, rather than one particular value, will be significant.

### III. BEHAVIOR OF $R_{sa}$ AND $R_r$ WITH ENERGY

The difficulties outlined in the previous section are not an encouraging introduction to the endeavor of looking for some kind of regularity in the energy dependence of  $R_{sa}$  and  $R_r$ . If there exists any such regularity, it should stand out more clearly when the same optical potential is used to describe the elastic scattering of a pair at different energies. Bond *et al.*<sup>12</sup> have fitted with the same Woods-Saxon (WS) potential the scattering of  $^{13}\text{C}$  by  $^{40}\text{Ca}$  at 40, 48, 60, and 68 MeV. With this potential we have computed  $R_{sa}$  and  $R_r$  not only at those energies but also at eleven other energies between 25 and 500 MeV. By this we do not pretend that the predictions of this particular potential should be good through all that range of energies. But these results should make easier to find the best functional form  $R_{sa}(E)$  and  $R_r(E)$  corresponding to a fixed potential, so that this behavior is checked later on against the available data for other pairs at a more limited range of energies.

Actually the 15 values computed for  $R_{sa}$  and  $R_r$  at  $25 \leq E \leq 500$  happen to be linear in  $E^{-1/3}$  and  $E^{-3/2}$ , respectively, with correlation coefficients very close to 1:

$$R_{sa} = 7.338 + 7.308E^{-1/3} \quad (r^2 = 0.9995), \quad (3)$$

$$R_r = 10.193 - 50.17E^{-3/2} \quad (r^2 = 0.9973). \quad (4)$$

We do not know of a mathematical or physical reason why these relations should be exact. Moreover, we doubt that the same potential can fit the experimental elastic scattering angular distribution at such a large variety of energies. But we shall see in the next section that the existing data do yield values of  $R_{sa}$  and  $R_r$  which can in most cases be approximated well by similar formulas:

$$R_{sa} = A + BE^{-1/3}, \quad (5)$$

$$R_r = C - DE^{-3/2}. \quad (6)$$

### IV. "EXPERIMENTAL" VALUES OF $R_{sa}$ AND $R_r$

The amount of good data sets (wide angular range with good resolution and small errors, which would determine the optical potential in an unam-

biguous way as much as possible) at an ample range of energies for a given pair of heavy ions is rather scanty and fairly recent. We survey in this section the optical model fits available to us and the resulting values of  $R_{sa}$  and  $R_r$ . We shall meet two types of optical potentials: the conventional WS fits on one hand, and, on the other hand, a large sample of fits published by Satchler and Love<sup>13</sup> with a folding real potential and a WS imaginary part. In the latter cases we have substituted for the real folded potential an analytical approximation

$$\begin{aligned} V(r) &= -V_0 s^n \exp(-s/a_R), \quad \text{if } s \geq na_R \\ &= -V_0 (na_R)^n e^{-n}, \quad \text{if } s \leq na_R, \end{aligned} \quad (7)$$

with

$$s = r - C_1 - C_2,$$

$$C_i = R_i - b^2/R_i, \quad b = 1 \text{ fm}$$

$$R_i = (1.13 + 0.0002A_i)A_i^{1/3}.$$

The validity of this approximation in the relevant region ( $1 < s < 4$ ) is pointed out in Ref. 13 and has been checked by us in some of these cases as well as in foldings with another effective interaction.<sup>14</sup> The optical model fits for each pair, and the corresponding values of  $R_{sa}$  and  $R_r$  are reported here in detail and summarized in Table I and Figs. 1 to 4.

<sup>6</sup>Li + <sup>40</sup>Ca at 28, 30, 34, 50.6, and 156 MeV from Ref. 13. The parameters in Eq. (7) that fit the folding are  $V_0 = 83.98$ ,  $n = 0.6881$ , and  $a_R = 0.6631$ . The imaginary potential used for the fit at 30 MeV has a much sharper boundary (smaller  $a_I$ ) than the neighboring energies and predicts a considerably smaller reaction cross section. The value of  $R_{sa}$  also is much too low and so this energy has been omitted in Fig. 1 as well as in the least square determination of the parameters of Eqs. (5) and (6).

<sup>9</sup>Be + <sup>28</sup>Si at seven different energies in the range 12–30 MeV. Bodek *et al.*<sup>15</sup> give three different WS fits with equal real and imaginary geometry common to all the energies:

$$(i) \quad V_0 = 20, \quad W_0 = 35.2, \quad r = 1.09, \quad a = 0.80,$$

$$(ii) \quad V_0 = 40, \quad W_0 = 69.7, \quad r = 0.95, \quad a = 0.82,$$

$$(iii) \quad V_0 = 100, \quad W_0 = 174.9, \quad r = 0.78, \quad a = 0.84.$$

None of them gives a rainbow effect at 12 MeV. All three give a very good fit to Eqs. (5) and (6), as can be seen in columns 6 and 9 of Table I and case (ii) in Fig. 3. Their predictions for  $R_{sa}$  and  $R_r$  differ  $\leq 0.1$  fm from one potential to another.

<sup>13</sup>C + <sup>40</sup>Ca at 40, 48, 60 and 68 MeV. These have been fitted with one and the same WS potential

TABLE I. Analytical fit to the energy dependence of the strong absorption radius,  $R_{sa} = A + BE^{-1/3}$ , and to the rainbow radius,  $R_r = C - DE^{-3/2}$ , and correlation coefficient of the fits,  $r^2$ . The center-of-mass energy  $E_{c.m.}^x$ , at which  $R_{sa} = R_r$ , and the percentage difference relative to the prediction  $E_{c.m.}^x = Z_1 Z_2 / 6.19$  are given in the last two columns.

Reaction	No. points <sup>a</sup>	Ref.	A	B	$r^2$	C	D	$r^2$	$E_{c.m.}^x$	$\Delta\%$
${}^6\text{Li} + {}^{40}\text{Ca}$	4(1)	b	6.637	7.420	0.999 1	9.778	31.94	0.942	16.8	73
${}^9\text{Be} + {}^{28}\text{Si}$	7	c	6.787	6.227	0.999 8	9.236	20.19	0.991 2	16.2	79
			6.691	6.324	0.999 7	9.156	21.65	0.994 5	16.7	85
			6.665	6.423	0.999 7	9.111	20.13	0.998 6	17.3	91
${}^{13}\text{C} + {}^{40}\text{Ca}$	15	d	7.338	7.308	0.999 5	10.193	50.17	0.997 3	19.5	0.6
${}^{15}\text{N} + {}^{27}\text{Al}$	4	e	6.996	6.557	0.999 7	9.994	41.87	0.999 99	11.9	-19
${}^{16}\text{O} + {}^{24}\text{Mg}$	5	f	6.594	7.652	0.999 98	9.478	39.48	0.999 3	15.6	0.6
${}^{16}\text{O} + {}^{26}\text{Mg}$	5	f	6.624	7.747	0.999 7	9.640	46.48	0.999 8	15.5	-0.1
		g	7.908	3.409	0.987	10.025	109.3	0.998 4	14.8	-4.6
${}^{16}\text{O} + {}^{28}\text{Si}$	4	g	7.782	4.451	0.889	10.156	124.1	0.997 4	17.1	-5.5
		b	6.871	7.848	0.979	9.701	62.42	0.997 3	20.1	11
${}^{16}\text{O} + {}^{30}\text{Si}$	4	g	7.932	4.227	0.949	10.268	120.1	0.999 5	16.9	-6.6
${}^{16}\text{O} + {}^{40}\text{Ca}$	5(2)	b	7.471	7.999	0.993	10.228	90.6	0.999 3	27.3	5.6
		h	7.765	6.781	0.999 6	10.320	98.3	0.999 3	24.9	-3.7
${}^{16}\text{O} + {}^{59}\text{Co}$	5(1)	b	8.318	7.062	0.961	10.640	117.2	0.999 9	36.9	5.7
${}^{16}\text{O} + {}^{208}\text{Pb}$	4	i	10.693	10.10	0.904	12.896	170.5	0.795	108	0.7
${}^{18}\text{O} + {}^{24}\text{Mg}$	5	f	6.782	7.543	0.999 96	9.492	44.43	0.998 8	17.0	9.6
${}^{20}\text{Ne} + {}^{40}\text{Ca}$	5(2)	j	8.400	7.896	0.971	10.970	193.6	0.918 7	36.2	12
${}^{40}\text{Ca} + {}^{40}\text{Ca}$	6	b	8.835	9.988	0.998 5	11.164	560.2	0.999 91	66.1	2.3
${}^{84}\text{Kr} + {}^{209}\text{Bi}$	2	k	13.569	6.084	1	14.407	2596	1	485	0.5

<sup>a</sup> Number of different energies for which an optical potential, fitted to experimental data, has been used to obtain  $R_{sa}$  and  $R_r$ . The points in parentheses are not considered in the fit of columns 4 to 9.

<sup>b</sup> Analytical approximation, Eq. (7), to folded potential of Ref. 13.

<sup>c</sup> Reference 15.

<sup>d</sup> Reference 12.

<sup>e</sup> Reference 16.

<sup>f</sup> Reference 17.

<sup>g</sup> Reference 18.

<sup>h</sup> Reference 20.

<sup>i</sup> Data averaged from Refs. 11, 13, and 21.

<sup>j</sup> Reference 22.

<sup>k</sup> Reference 23.

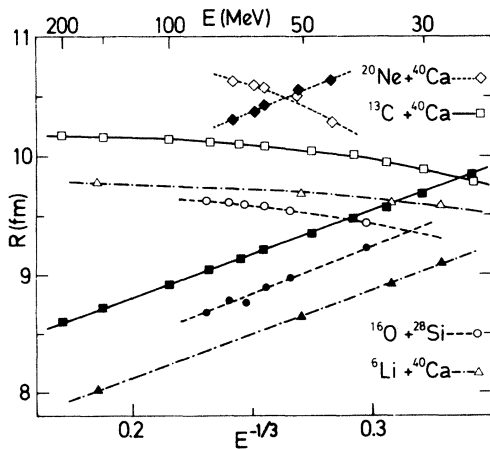


FIG. 1. Strong absorption radius  $R_{sa}$  (black symbols) and a rainbow distance  $R_r$  (open symbols) as a function of the projectile energy. The curves are least square fits  $R_{sa} = A + B^{-1/3}$  and  $R_r = C - DE^{-3/2}$ .

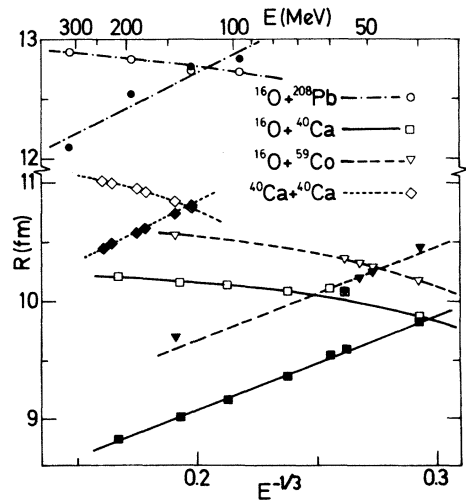


FIG. 2. Strong absorption radius  $R_{sa}$  (black symbols) and rainbow distance  $R_r$  (open symbols) as a function of the projectile energy. The curves are least square fits  $R_{sa} = A + BE^{-1/3}$  and  $R_r = C - D^{-3/2}$ .

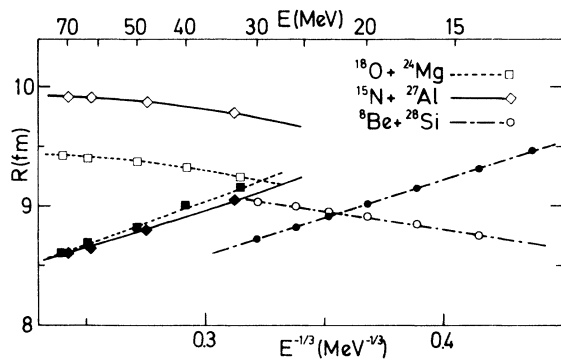


FIG. 3. Strong absorption radius  $R_{sa}$  (black symbols) and rainbow distance  $R_r$  (open symbols) as a function of the projectile energy. The curves are least square fits  $R_{sa} = A + BE^{-1/3}$  and  $R_r = C - DE^{-3/2}$ .

by Bond *et al.*<sup>12</sup> As we have explained in the previous section, a much wider range of energies without reference to experimental data has been considered for this potential and is shown in Fig. 1.

$^{15}\text{N} + ^{27}\text{Al}$  at four energies between 33 and 70 MeV. These have been fitted with a six parameter WS potential by Prosser *et al.*<sup>16</sup> and the resulting values of the strong absorption and rainbow radii follow very accurately the proposed  $E$  dependence of Eqs. (5) and (6). They are shown in Fig. 3.

$^{16}\text{O} + ^{24,26}\text{Mg}$  (Fig. 4) and  $^{18}\text{O} + ^{24}\text{Mg}$  (Fig. 3) at five energies between 32 and 72 MeV. These have been fitted each pair to an energy-independent six-parameter WS potential by Tabor *et al.*<sup>17</sup> Fortune *et al.*<sup>18</sup> have published another WS fit to  $^{16}\text{O} + ^{26}\text{Mg}$  at four energies between 35 and 50 MeV with the real and imaginary depths linear in energy. In this case the fits (5) and (6) are less accurate.

$^{16}\text{O} + ^{28,30}\text{Si}$ . Fortune *et al.*<sup>18</sup> have published the same type of WS fits also for these reactions at the same energies 35–50 MeV, and again the energy dependence of the potential makes formula (5) less accurate.  $^{16}\text{O} + ^{28}\text{Si}$  has also been fitted by Satchler and Love at eight energies from 37.7 to 215.2 MeV and their folding is approximated by Eq. (7) with  $V_0 = 129.06$ ,  $n = 1.1825$ , and  $a_R = 0.5031$ . The values of  $R_{sa}$  (and to some extent of  $R_r$ ) predicted by this potential at the two highest energies are in strong disagreement with the behavior followed at lower energies and have not been considered in Fig. 1 or in the fits of Eqs. (5) and (6). But one can see<sup>19</sup> that the  $\chi^2$  of the folding potentials at these energies is substantially higher than with a WS potential.

$^{16}\text{O} + ^{40}\text{Ca}$  at seven energies from 40 to 214.1 MeV. These are also included in the folding potentials of Ref. 13 and are here approximated with  $V_0 = 135.93$ ,  $n = 1.1282$ , and  $a_R = 0.5174$ . Among the

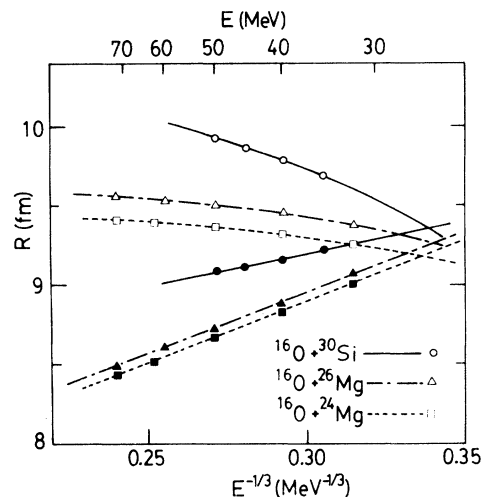


FIG. 4. Strong absorption radius  $R_{sa}$  (black symbols) and rainbow distance  $R_r$  (open symbols) as a function of the projectile energy. The curves are least square fits  $R_{sa} = A + BE^{-1/3}$  and  $R_r = C - DE^{-3/2}$ .

different alternatives offered by the authors we have preferred, whenever possible, those with the same normalization. At 55.6 and 60 MeV it has not been possible: These points in Fig. 2 are slightly out of the smooth curve and have not been used in the fit. Also Vigdor *et al.*<sup>20</sup> have published several WS fits to this reaction at five energies between 55.6 and 214.1 MeV. We have chosen the one called 2a, which is common to all the energies and gives a more smooth behavior for our curves.

$^{16}\text{O} + ^{59}\text{Co}$  at six energies ranging from 40 to 141.7 MeV. These are also included in the folded potentials available to us. This folding has been approximated with  $V_0 = 139.25$ ,  $n = 1.1138$ , and  $a = 0.5226$ . Data at 45.5 MeV require a different renormalization and this makes the values of  $R_{sa}$  and  $R_r$  out of a smooth behavior; so they have not been used in the fit of Eqs. (5) and (6), nor in Fig. 2.

$^{16}\text{O} + ^{208}\text{Pb}$ . This pair has been measured at many energies and studied in many ways. The folded potential, applied to data at 129.5, 192, and 312.6 MeV, has been approximated here with  $V_0 = 141.5$ ,  $n = 1.0081$ , and  $a_R = 0.5499$ . Data at 129.5 and 192 MeV were also fitted by Ball *et al.*<sup>21</sup> with four parameter WS potentials. A reasonable choice (or average, in the case of 129.5 MeV) of these various possibilities has been plotted in Fig. 2 and used for the fits (5) and (6). Videbaek *et al.*<sup>11</sup> have measured and fitted with WS potentials this pair at many close energies in the interval 80–96 MeV. They fix the potential depth and vary the radius. The resulting fluctuations in the values

of  $R_{sa}$  and  $R_r$ , due to the potential ambiguity, are rather meaningless in such a narrow energy interval, and we have taken an average value of these quantities associated to an average energy. This pair also has been considered by Vaz *et al.*<sup>24</sup> They explicitly study the energy dependence of the strong absorption radius and the rainbow radius for a given potential which is supposed to be valid for all the energies, and they found  $R_r > R_{sa}$  at higher energies, the crossing point being about 90 MeV projectile energy for an optimum imaginary radius  $r_I = 1.32$  or 170 MeV for a possible  $r_I = 1.42$  (see Fig. 2 of Ref. 24). In an associated paper Vaz and Alexander<sup>25</sup> suggest that this crossing energy for other pairs may depend on the strength of the Coulomb field, an idea which we shall confirm in the next section in a more quantitative way.

<sup>20</sup>Ne + <sup>40</sup>Ca at seven energies from 44.1 to 70.4 MeV. These have been measured and fitted by Van Sen *et al.*<sup>22</sup> with WS potentials of constant depth and energy-dependent geometry. Two of the energies (48.9 and 55.7 MeV) give values of the radii a little below the smooth curve, and have not been used in the fit nor plotted in Fig. 1.

<sup>40</sup>Ca + <sup>40</sup>Ca at six energies from 143.6 to 240 MeV. These are included among the folded potentials of Ref. 13 and approximated here with  $V_0 = 162.67$ ,  $n = 1.1313$ , and  $a_R = 0.5234$ . Since they have the same renormalization and imaginary potential at all energies, we expect and find a regular behavior in  $R_{sa}(E)$  and  $R_r(E)$ .

<sup>84</sup>Kr + <sup>209</sup>Bi. We have data and WS potentials fitted to them at two energies only<sup>23</sup> (600 and 712 MeV) so that the curves are determined exactly, and they happen to cross between these two energies.

### V. COULOMB DEPENDENCE OF THE CROSSING ENERGY

In the results of the previous section one can see that  $R_r > R_{sa}$  at high energies and  $R_{sa} > R_r$  at low energies (frequently extrapolated from existing data). The crossing energy, such that  $R_{sa}(E^x) = R_r(E^x)$ , was suspected to be related to the strength of the Coulomb field.<sup>25</sup> In order to study this possible connection in a quantitative way we have plotted in Fig. 5 the center-of-mass crossing energy,  $E_{c.m.}^x = E^x M_2 / (M_1 + M_2)$ , as a function of  $Z_1 Z_2$ . A log-log scale has been chosen for a better distribution of the points. At the same time it is apparent that, with the exception of the pairs including <sup>6</sup>Li or <sup>9</sup>Be projectiles (not shown in the plot), all the others correspond rather well with a straight line with 45° slope. This means a proportionality between  $E_{c.m.}^x$  and  $Z_1 Z_2$

$$E_{c.m.}^x = Z_1 Z_2 / 6.19. \quad (8)$$

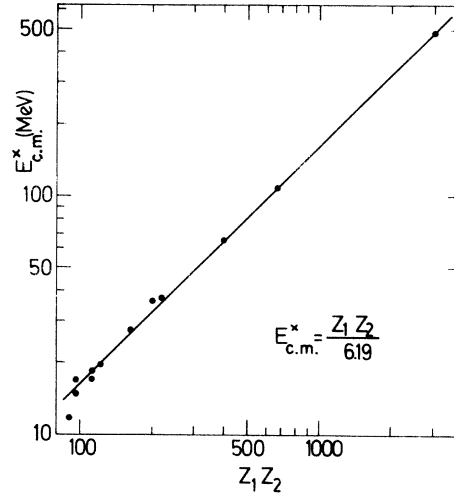


FIG. 5. The crossing energy, where  $R_{sa} = R_r$ , measured in the center-of-mass system as a function of  $Z_1 Z_2$ .

In the last two columns of Table I we give the experimental value of  $E_{c.m.}^x$ , obtained by equating the fits

$$A + B(E^x)^{-1/3} = C - D(E^x)^{-3/2}$$

and the percentage deviation of this experimental value from the prediction of Eq. (8). This deviation is no more than a few percent with the exception of the two lighter projectiles, which have not been considered in the fit (8). They once more do not altogether behave like heavy ions.

### VI. CONCLUDING REMARKS

We have found empirically analytical expressions that describe quite accurately the variation with energy of the strong absorption radius, Eq. (5), and the Coulomb rainbow radius, Eq. (6), corresponding to a complex optical potential of the Woods-Saxon type. Such analytical expressions seem to be applicable also to values of  $R_{sa}$  and  $R_r$  corresponding to optical potentials actually fitted to the existing data of elastic scattering for every given pair of heavy ions at different energies, at least when a constant (or smoothly  $E$ -dependent) potential is used for all the energies and the same pair.

This conclusion is arrived at only after a certain selection of the data is made. This fact weakens the strength of the conclusion but is justified by the difficulties pointed out in Sec. II. The relative amount of data that fits in our scheme is large enough to make it meaningful. Our functions  $R_{sa}(E)$  and  $R_r(E)$  cross at a point which, if mea-

sured in the c.m. frame of reference, is proportional to  $Z_1 Z_2$ , as indicated by Eq. (8). This result suggests that refraction prevails over absorption in determining the elastic scattering angular distribution above such crossing energy, while the contrary would be the case at lower energies.

## ACKNOWLEDGMENTS

We are grateful to G. R. Satchler for communicating to us many experimental data and his folding potentials. Financial help from the Instituto de Estudios Nucleares, Madrid, is also acknowledged.

- 
- <sup>1</sup>E. Rutherford, *Philos. Mag.* **21**, 669 (1911).  
<sup>2</sup>K. W. Ford and J. A. Wheeler, *Ann. Phys. (N. Y.)* **7**, 259 (1959).  
<sup>3</sup>D. A. Goldberg, *Phys. Lett.* **55B**, 59 (1975); *Proceedings of the Second Louvain-Cracow Seminar on the Alpha-Nucleus Interaction, Louvain, 1978*, edited by G. Grégoire and K. Grotowski (Université de Louvain, Louvain-la-Neuve), p. 41; D. A. Goldberg and S. M. Smith, *Phys. Rev. Lett.* **29**, 500 (1972).  
<sup>4</sup>R. da Silveira, *Phys. Lett.* **45B**, 211 (1973).  
<sup>5</sup>W. E. Frahn, *Ann. Phys. (N. Y.)* **72**, 524 (1972); W. E. Frahn and D. H. E. Gross, *ibid.* **101**, 520 (1976).  
<sup>6</sup>R. C. Fuller, *Phys. Rev. C* **12**, 1561 (1975).  
<sup>7</sup>G. R. Satchler, in *Sixth INS Summer School on Nuclear Physics, Dogashima, Japan, 1978* (unpublished).  
<sup>8</sup>M. Lozano and G. Madurga, *Nucl. Phys.* **A334**, 349 (1980).  
<sup>9</sup>R. E. Langer, *Phys. Rev.* **51**, 669 (1937).  
<sup>10</sup>G. R. Satchler, in *Proceedings of the International Conference on Reactions between Complex Nuclei, Nashville, Tennessee, 1974*, edited by R. L. Robinson, F. K. McGowan, J. B. Ball, and J. H. Hamilton (North-Holland, Amsterdam, 1974), Vol. II, p. 171.  
<sup>11</sup>F. Videbaek, R. B. Goldstein, L. Grodzins, S. G. Steadman, T. A. Belote, and J. D. Garrett, *Phys. Rev. C* **15**, 954 (1977).  
<sup>12</sup>P. D. Bond, J. D. Garrett, O. Hansen, S. Kahana, M. J. LeVine, and A. Z. Schwarzschild, *Phys. Lett.* **47B**, 231 (1973).  
<sup>13</sup>G. R. Satchler and W. G. Love, *Phys. Rep.* **C55**, 183 (1979).  
<sup>14</sup>F. J. Viñas, G. Madurga, and M. Lozano, *Phys. Rev. C* **23**, 780 (1981).  
<sup>15</sup>K. Bodek, M. Hugi, J. Lang, R. Müller, E. Ungricht, K. Jankowski, W. Zipper, L. Jarczyk, A. Strazałkowski, G. Willim, and H. Witafa, *Nucl. Phys.* **A339**, 353 (1980).  
<sup>16</sup>F. W. Prosser, Jr., R. A. Racca, K. Daneshvar, D. F. Geesaman, W. Henning, D. G. Kovar, K. E. Rehm, and S. L. Tabor, *Phys. Rev. C* **21**, 1819 (1980).  
<sup>17</sup>S. L. Tabor, D. F. Geesaman, W. Henning, D. G. Kovar, K. E. Rehm, and F. W. Prosser, Jr., *Phys. Rev. C* **17**, 2136 (1978).  
<sup>18</sup>H. T. Fortune, A. Richter, R. H. Siemssen, and J. L. Yntema, *Phys. Rev. C* **20**, 648 (1979).  
<sup>19</sup>G. R. Satchler, M. L. Halbert, N. M. Clarke, E. E. Gross, C. B. Fulmer, A. Scott, D. Martin, M. D. Cohler, D. C. Hensley, C. A. Ludemann, J. G. Cramer, M. S. Zisman, and R. M. DeVries, *Nucl. Phys.* **A298**, 313 (1978).  
<sup>20</sup>S. E. Vigdor, D. G. Kovar, P. Sperr, J. Mahoney, A. Menchaca-Rocha, C. Olmer, and M. S. Zisman, *Phys. Rev. C* **20**, 2147 (1979).  
<sup>21</sup>J. B. Ball, C. B. Fulmer, E. E. Gross, M. L. Halbert, D. C. Hensley, C. A. Ludemann, M. J. Saltmarsh, and G. R. Satchler, *Nucl. Phys.* **A252**, 208 (1975).  
<sup>22</sup>N. Van Sen, R. Darves-Blanc, J. C. Gondrand, and F. Merchez, *Phys. Rev. C* **20**, 969 (1979).  
<sup>23</sup>J. R. Birkelund, J. R. Huizenga, H. Freiesleben, K. L. Wolf, J. P. Unik, and V. E. Viola, Jr., *Phys. Rev. C* **13**, 133 (1976).  
<sup>24</sup>L. C. Vaz, J. M. Alexander, and E. H. Auerbach, *Phys. Rev. C* **18**, 820 (1978).  
<sup>25</sup>L. C. Vaz and J. M. Alexander, *Phys. Rev. C* **18**, 833 (1978).